Standardized Universal Pulse: a fast RF calibration approach to improve flip angle accuracy in parallel transmission

Caroline Le Ster[1], Franck Mauconduit[1], Aurélien Massire[2], Nicolas Boulant[1], and Vincent Gras*[1]

[1]Université Paris-Saclay, CEA, CNRS, BAOBAB, NeuroSpin, 91191, Gif-sur-Yvette, France

[2]Siemens Healthineers SAS, 93527, Saint-Denis, France

*Corresponding author: Vincent Gras, Université Paris-Saclay, CEA, CNRS, BAOBAB, NeuroSpin, F-91191, Gif-Sur-Yvette, France. E-mail: vincent.gras@cea.fr

Abstract

Purpose: In parallel transmission (pTX), subject-tailored RF pulses allow achieving excellent flip angle (FA) accuracy but often require computationally extensive online optimisations, precise characterisation of the the static field (ΔB_0) and the transmit RF field (B_1^+) distributions. This costs time and requires expertise from the MR user. Universal Pulses (UP) have been proposed to reduce this burden, yet, with a penalty in FA accuracy. This study introduces the concept of standardised universal pulses (SUP), where pulses are designed offline and adjusted to the subject through a fast online calibration scan.

Methods: A SUP is designed offline using a so-called standardised database, wherein each B_1^+ map has been normalised to a reference transmit RF field distribution. When scanning a new subject, a 3-slice B_1^+ acquisition (scan time < 10 s) is performed and used to adjust the SUP to the subject through a linear transform. SUP performance was assessed at 7T with simulations by computing the FA-normalised root mean square error (FA-NRMSE) and the FA profile stability as measured by the average and coefficient of variation of the FA across 15 control subjects, along with *in vivo* experiments using an MP2RAGE sequence implementing the SUP variant for the FLASH readout.

Results: Adjusted SUP improved the FA-NRMSE (8.8 % for UP versus 7.1 % for adjusted SUP). Experimentally, *in vivo*, this translated in an improved signal homogeneity and more accurate T_1 quantification using MP2RAGE.

Conclusion The proposed SUP approach improves excitation accuracy (FA-NRMSE) while preserving the same offline pulse design principle as offered by UPs.

Keywords: ultra-high field, parallel transmission, RF pulse design, MP2RAGE, universal pulse

Word count: 4500

Introduction

In MRI at ultra-high field (UHF), radio-frequency (RF) excitation profiles produced by the RF transmit coil suffer from spatial inhomogeneities due to destructive interferences occurring within the body. They show reproducible patterns (typically low signal in the temporal lobe and cerebellum for head imaging at 7T), but present to a certain degree an inter-subject and inter-session variability that depends on the position in the coil, morphology and composition (1). To mitigate this effect, the use of parallel transmission (pTX) with an array of local transmit coils has been shown to be a very efficient approach (2–5). In pTX, the amplitudes and phases of the pulses transmitted by the channels of the array can be modulated independently to homogenise the excitation profile over the volume of interest, provided the actual static field offset (ΔB_0) and the transmit RF field (B_1^+) distributions are known. For non-selective excitations, various approaches have been proposed to design optimised RF and magnetic field gradient (MFG) waveforms, in particular with k_T-points (6), SPINS (7) and recently GRAPE (8). The design of such subject-tailored pulses results in very homogeneous RF excitation profiles, at the cost of the scan time required to map ΔB_0 and B_1^+ fields and to design the pulses, along with a certain expertise from the MR user. Strategies have been proposed to speed up and ease the acquisition workflow using either fast B_1^+ mapping (9), fast pulse computation (10) or universal approaches (11–14). Within the Universal Pulse (UP) framework, the pulse design step is performed offline so that no time or expertise is required during the scanning session. UPs make use of the reproducibility of the ΔB_0 and B_1^+ distributions across subjects to design a pulse that homogenises the excitation profiles simultaneously across all subjects of a so-called design database. UPs can then be applied to new subjects without further calibration and with good excitation performance, albeit with some performance penalty compared to the subject-tailored pulse design approach. For many imaging applications, UP performance for brain imaging at 7T appears to be sufficient (12). It has also shown robustness across subjects, though some variability remains due to differences in head morphology, placement and composition. As a result, an UP designed to realise a given uniform flip angle (FA) value across the entire brain can occasionally produce a FA distribution whose average value across the brain can deviate significantly from the expected value. For instance, in (15), the average deviation from the nominal FA could reach up to 10 % over the brain in some volunteers.

In this study, a new UP design approach is introduced to improve the stability of the

excitation pattern across subjects through a standardisation of the pulse design database and a session-specific fast calibration scan. It relies on the normalisation of the N_c-dimensional B_1^+ distribution of the subject, where N_c is the number of transmit channels (8 in this work) to map the B_1^+ amplitudes and phases of the subject to a *reference* B_1^+ distribution. This step is performed through a linear transformation with an $N_c \times N_c$ complex adjustment matrix, which is meant to account for variations in coil loading and coupling between transmitters. This transformation is applied on every subject of the database to produce a so-called *standardised* design database; a universal pulse designed on the standardized design database is then called a standardised UP (SUP). This approach imposes a calibration step during the MRI exam, where the adjustment matrix of the subject is estimated from a fast B_1^+ scan (< 10 s) (16–18). However, as for UPs, SUPs do not require online pulse design, so that only a fast calibration procedure is performed online, resulting in a simplified workflow and shorter processing times compared to a subject-tailored approach.

The aim of the current study was to assess the performance of adjusted SUPs by comparison to UP and subject-tailored pulses in the small tip angle regime, with non-selective pulses as used for spin excitation in the magnetization prepared two rapid acquisition gradient echoes (MP2RAGE) sequence (19, 20). A GRAPE algorithm was chosen for the pulse design to allow for short pulse duration and improved robustness to off-resonance artefacts (8). UP, SUP and subject-tailored pulse performances were compared in terms of the normalised root mean square error (FA-NRMSE) and coefficient of variation of the simulated FA profile, along with *in vivo* acquisitions at 7T. The use of the same inversion pulse, in addition to the MP2RAGE inherent robustness versus receive profile variations, proton-density and T_2^* contrasts make the comparison between the three pulse design strategies relatively straightforward. The two inversion contrasts of the MP2RAGE were further used to perform T_1 quantification so that T_1 maps obtained with adjusted SUP were compared to the ones obtained with UP with a B_1^+ correction (14, 21).

Theory

Universal Pulse design

Let us consider a design database consisting of ΔB_0 and B_1^+ brain field maps acquired over N_s subjects with N_c transmit coils ($\Delta B_{0,S:1}$, $B_{1,S:1}^+$, $\cdots$, $\Delta B_{0,S:N_s}$, $B_{1,S:N_s}^+$). For each subject,

ΔB_0 and B_1^+ brain field maps are defined over a set of positions $\mathcal{R}_{S:n}$ which correspond to the brain volume. For simplicity, we represent ΔB_0 and B_1^+ as $M_n \times 1$ and $M_n \times N_c$ matrices (ΔB_0 being real and B_1^+ complex), where each row of the matrix corresponds to one voxel in $\mathcal{R}_{S:n}$ and where $M_n = |\mathcal{R}_{S:n}|$ represents the number of elements of $\mathcal{R}_{S:n}$. Let P_{UP} be a Universal Pulse defined by its RF and MFG waveforms: $U_{UP}(t) \in \mathbb{C}^{1\times N_c}$ in Volt and $G_{UP}(t) \in \mathbb{R}^3$ in T/m, respectively. The universal pulse P_{UP}, denoted by $P_{UP} = U_{UP} \odot G_{UP}$, is designed offline on the design database with a minimisation of the average FA-NRMSE across subjects:

$$J = \left(\frac{1}{N_s} \sum_{n=1}^{N_s} J_n^2 \right)^{1/2}, \tag{1}$$

where:

$$J_n^2 = \frac{1}{\alpha_t^2 M_n} \sum_{r \in \mathcal{R}_{S:n}} (\alpha_n(r) - \alpha_t)^2 \tag{2}$$

and where α_t is the targeted FA and $\alpha_n(r)$ is the actual FA simulated at position r for subject n. The latter is given in the STA approximation by (22):

$$\alpha_n(r) = 2\pi\gamma \left| \int_{t=0}^{T} U(t) \cdot B_{1,S:n}^+(r) e^{ik(t)\cdot r} e^{-i2\pi\gamma \Delta B_0(r)(T-t)} dt \right| \tag{3}$$

where $|z|$ corresponds to the magnitude of z, T to the pulse duration in s, $\gamma = 42.57$ MHz/T to the gyromagnetic ratio of the proton and k(t) to the transmit k-space trajectory in m^{-1}:

$$k(t) = -2\pi\gamma \int_{t'=t}^{T} G(t') dt'. \tag{4}$$

We note in Equation [3] that the product $U(t) \cdot B_{1,S:n}^+(r)$ is a matrix product where the individual TX channel contributions are summed together.

Standardised Universal Pulse design

In a normalisation process of the design database called *standardisation*, every B_1^+ map of the database is expressed as the linear transform of a reference, while the ΔB_0 maps are left unchanged. The first step of this process is thus to define a reference $B_{1,ref}^+$ over the region of interest $\mathcal{R}_{ref}$. Let $\mathcal{I}(r)$ represent the set of subjects where $\mathcal{R}_{S:n}$ is defined (i.e. $\mathcal{I}(r) = \{1 \leq n \leq N_s, r \in \mathcal{R}_{S:n}\}$). $B_{1,ref}^+$ is taken here as the average B_1^+ over $\mathcal{R}_{ref}$, chosen as

the set of voxels where $\mathcal{R}_{\mathrm{S:n}}$ is defined in at least half of the subjects:

$$\begin{cases} \mathrm{B}^{+}_{1,\mathrm{ref}} = \frac{1}{|\mathcal{I}(\mathrm{r})|} \sum_{\mathrm{n}\in\mathcal{I}(\mathrm{r})} \mathrm{B}^{+}_{1,\mathrm{S:n}}, \\ \mathcal{R}_{\mathrm{ref}} = \{\mathrm{r}\ ;\ |\mathcal{I}(\mathrm{r})| \geq \mathrm{N_s}/2\}, \end{cases} \tag{5}$$

where $|\mathcal{I}(r)|$ is the cardinal of $\mathcal{I}(r)$. The second step is to compute the dimensionless $\mathrm{N_c} \times \mathrm{N_c}$ adjustment matrix $\mathrm{L_n}$ that fits $\mathrm{B}^{+}_{1,\mathrm{S:n}}$ to $\mathrm{B}^{+}_{1,\mathrm{Ref}}$ as the solution to the least-squares problem:

$$\mathrm{L_n} = \mathrm{argmin}_{\mathrm{L}\in\mathbb{C}^{\mathrm{N_c}\times\mathrm{N_c}}} \left\| \mathrm{B}^{+}_{1,\mathrm{S:n}}\left(\mathcal{R}_{\mathrm{S:n}} \cap \mathcal{R}_{\mathrm{ref}}\right) - \mathrm{L}\mathrm{B}^{+}_{1,\mathrm{ref}}\left(\mathcal{R}_{\mathrm{S:n}} \cap \mathcal{R}_{\mathrm{ref}}\right) \right\|^2_{\mathrm{Fro}} \tag{6}$$

where $\|.\|_{\mathrm{Fro}}$ represents the Fröbenius norm and, for any set of positions $\mathrm{A} \in \mathcal{R}_{\mathrm{S:n}}$, $\mathrm{B}^{+}_{1,\mathrm{S:n}}(\mathrm{A})$ denotes the submatrix of $\mathrm{B}^{+}_{1,\mathrm{S:n}}$ containing the rows that correspond to A. The standardised RF field of this subject, $\tilde{\mathrm{B}}^{+}_{1,\mathrm{S:n}}$, is then defined as:

$$\tilde{\mathrm{B}}^{+}_{1,\mathrm{S:n}}\left(\mathcal{R}_{\mathrm{S:n}}\right) = \mathrm{L_n^{-1}} \mathrm{B}^{+}_{1,\mathrm{S:n}}\left(\mathcal{R}_{\mathrm{S:n}}\right) \tag{7}$$

This operation is repeated for every subject of the design database. A standardised UP, $\mathrm{P_{SUP}} = \mathrm{U_{SUP}} \odot \mathrm{G_{SUP}}$, is an UP designed on the above-defined standardised database. As the databases used to design the UP and the SUP are different (i.e. "raw" versus standardised), the resulting RF and MFG waveforms of these pulses differ in general.

SUP adjustment

In contrast to $\mathrm{P_{UP}}$ which can be applied to new subjects without any calibration, a calibration step is required to adjust $\mathrm{P_{SUP}}$ to the subject (see Figure 1). This calibration consists in estimating the session-specific adjustment matrix $\mathrm{L_n}$ from the subject B^{+}_{1} field (rewritten as a matrix) with Equation [6], and then applying the linear transform to the SUP RF waveforms, while its MFG waveforms are left unchanged:

$$\begin{cases} \mathrm{U_{adjSUP}}(\mathrm{t}) = \mathrm{U_{SUP}}(\mathrm{t})\mathrm{L}^{-1} \\ \mathrm{G_{adjSUP}}(\mathrm{t}) = \mathrm{G_{SUP}}(\mathrm{t}) \end{cases} \tag{8}$$

The adjusted standardised pulse $\mathrm{P_{adjSUP}} = \mathrm{U_{adjSUP}} \odot \mathrm{G_{SUP}}$ thus obtained is defined as:

$$\mathrm{P_{adjSUP}} = \left(\mathrm{U_{SUP}}\mathrm{L}^{-1}\right) \odot \mathrm{G_{SUP}} \triangleq \mathrm{P_{SUP}}/\mathrm{L} \tag{9}$$

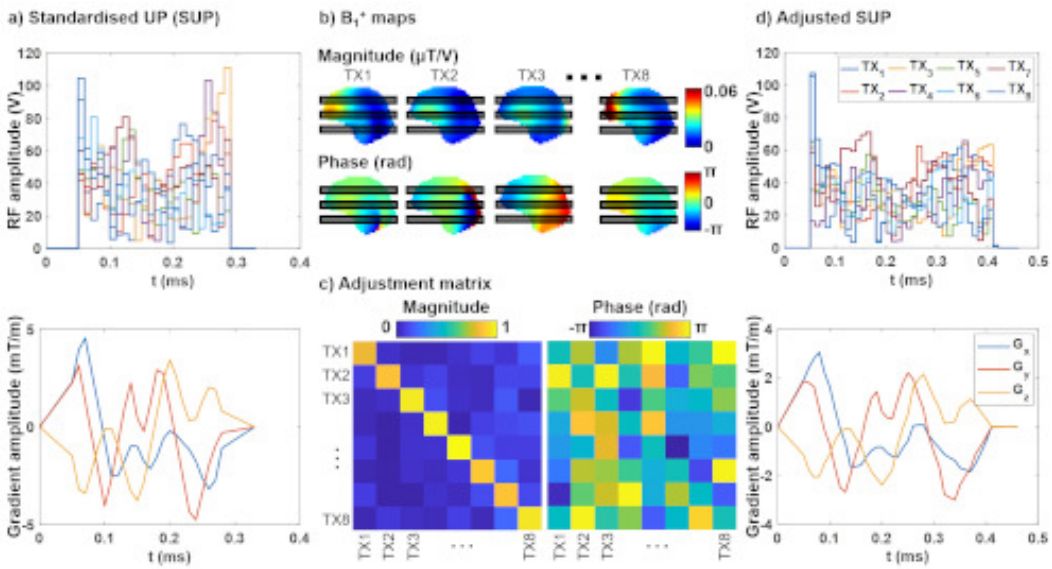

Figure 1: Methodology of the adjusted standardised universal pulse (SUP) approach. a) The design database that has been normalised to a reference (standardised database) is used to design a SUP with the same formalism as for UP. This pulse design step is performed offline. b to d) Calibration steps performed during the scanning session to adjust the SUP to the subject. b) During the scan, a subsampled B_1^+ map is acquired with e.g. 3 axial slices equally spaced over the brain, as represented here with dark lines. c) An $N_c \times N_c$ matrix is then estimated by fitting the B_1^+ map to the reference. The magnitude of the adjustment matrix is close to the identity matrix, while diagonal phase terms are close to 0 rad. d) The RF waveforms of the SUP are multiplied by the adjustment matrix, while its gradient waveforms are initially left unchanged. MFG ramps are added and, if needed, the RF and gradient waveforms are scaled and re-interpolated to match scanner and SAR limits. The adjusted SUP can then be run on the MR system.

To understand this, we insert U_{adjSUP} and G_{adjSUP} in Equation [3] and examine the product $U_{adjSUP} \cdot B_1^+$. From equations (7) and (8), we have:

$$U_{adjSUP} \cdot B_1^+ = \left(U_{SUP} L^{-1}\right)\left(L\tilde{B}_1^+\right) = U_{SUP}\tilde{B}_1^+ \tag{10}$$

i.e. the action of P_{adjSUP} on B_1^+ is equivalent to the action of P_{SUP} on $\tilde{B}_1^+$.

Since the least-squares problem for computing L is overdetermined ($N_c \times N_c \ll M_n$ complex numbers to fit), it can be estimated from a subsampled B_1^+ map, e.g. from a partial coverage of the brain with 3 slices. This allows achieving a significant reduction of the scan time as compared to a full-brain coverage B_1^+ mapping protocol.

A verification is then performed to ensure that the adjusted SUP fits scanner and SAR limits (maximal energy per channel $E_{ch,max}$, average energy summed over channels $E_{tot,max}$ and peak power limit V_{max}). Let λ be the pulse scaling parameter defined as:

$$\lambda = \max\{E_{ch}/E_{ch,max}; E_{tot}/E_{tot,max}; V/V_{max}\} \tag{11}$$

If $\lambda > 1$ (i.e. any of the above limits is exceeded), the pulse length is scaled according to the equation:

$$\begin{cases} U_{adjSUP}(t) = \frac{1}{\lambda} \times U_{adjSUP}(\lambda t), \\ G_{adjSUP}(t) = \frac{1}{\lambda} \times G_{adjSUP}(\lambda t) \end{cases} \tag{12}$$

The pulse is then reinterpolated on a 10 μs raster time to comply with the pulse definition imposed by the scanner's hardware.

Methods

Pulse design

MP2RAGE UP and SUP excitation pulse

A small tip angle (max 8°) universal pulse (UP) and standardised universal pulse (SUP) were designed with the GRAPE algorithm (8). The designs of these pulses were performed offline on a design database comprising the brain field maps of 20 subjects that were collected in a previous study (11). The UP was designed on this "raw" database, while the SUP was designed on the standardised database according to the processing steps described in the Theory section.

The UP and the SUP were computed using the active-set algorithm available in Matlab (R2020a release, the Mathworks, Natick, MA, USA). The optimisation algorithm was initialised with $G(t) = 0$ and U(t) obtained using the variable exchange method (23, 24). These pulses were 240 µs long and the design constraints to account for scanner and SAR limits were (at the coil plug): energy per channel $E_{ch,max} = 15$ mW, average energy $E_{tot,max} = 90$ mW, RF peak power limit V_{max}= 165 V, maximum slew rate = 180 T/m/s. The number of iterations was limited to 2×10^3 and the discretization time was set to 10 μs. As the GRAPE optimisation can lead to a gradient waveform with non-vanishing initial and final values, MFG ramps of 50 μs were added at the beginning and the end of the UP and the SUP to match slew rate constraints.

MP2RAGE UP inversion pulse

A 7 ms-long 180° GRAPE UP was design offline on the "raw" database using the active-set algorithm, and taking a low-amplitude hyperbolic-secant pulse for the initialisation of the RF waveform. Here, a discretization time of 40 μs was used, the RF energy was limited to 900 mW per channel and 6 W total, and the maximum RF voltage was constrained to not exceed V_{max}= 165 V. For the design of the inversion pulse, an additional ΔB_0 weighting term in the objective function to increase inversion accuracy in voxels exhibiting strong ΔB_0 excursions (8).

Validation in simulation

Excitation performance of the MP2RAGE excitation pulse was assessed in terms of fidelity to the targeted FA for the UP, the adjusted SUP and subject-tailored pulses using a control database of ΔB_0 and B_1^+ maps acquired over 15 subjects different from those used in the design database. These maps were acquired in a previous study (8, 11).

For FA simulations, the UP was applied to the subjects of the database without further adjustments. For the SUP, $B^+_{1,S:n}$ and $B^+_{1,ref}$ were first subsampled to match the B_1^+ sampling pattern chosen for *in vivo* experiments (3 axial slices equally spaced over the brain and distant by 3 cm, see Figure [1]b). The adjustment matrix L_n defined by Equation [6] was then computed by pseudo-inverse (Figure 1c). The SUP was finally adjusted to the subjects and scaled using Equations [8] and [12]. For comparison with the subject-tailored approach, a subject-specific pulse was designed for every subject of the control database using the same constraints as for UP and SUP, and using the UP for the initialisation of the RF and MFG waveforms (10).

The simulation results were analysed in terms of i) the average FA across the subjects and ii)

the coefficient of variation (CV) of the FA, defined for every subject n and for every voxel in the domain $\mathcal{R}_{\mathrm{S:n}}$ as:

$$\begin{cases} \mu = \frac{1}{\mathrm{N_s}} \sum_{\mathrm{n}=1}^{\mathrm{N_s}} \alpha_{\mathrm{n}} \\ \mathrm{CV} = \frac{1}{\mu} \sqrt{\frac{\sum_{\mathrm{n}=1}^{\mathrm{N_s}} (\alpha_{\mathrm{n}} - \mu)^2}{\mathrm{N_s}}} \end{cases} \tag{13}$$

In order to evaluate the importance of the off-diagonal elements of the adjustment matrix on SUP performance, an alternative definition of the adjustment matrix was investigated wherein the off-diagonal coefficients of the adjustment matrix were forced to zero:

$$\mathrm{L_{n,D}} = \mathrm{diag}(\delta_{\mathrm{n}}) \tag{14}$$

where

$$\delta_n = \mathrm{argmin}_{\delta \in \mathbb{C}^{\mathrm{N_c} \times 1}} \left\| \mathrm{B}^{+}_{1,\mathrm{S:n}} \left(\mathcal{R}_{\mathrm{S:n}} \cap \mathcal{R}_{\mathrm{ref}} \right) - \mathrm{diag}(\delta) \mathrm{B}^{+}_{1,\mathrm{ref}} \left(\mathcal{R}_{\mathrm{S:n}} \cap \mathcal{R}_{\mathrm{ref}} \right) \right\|^2_{\mathrm{Fro}} \tag{15}$$

where $\mathrm{diag}(\delta)$ denotes the $\mathrm{N_c} \times \mathrm{N_c}$ matrix whose diagonal coefficients are $\delta_1, .., \delta_{\mathrm{N_c}}$. These two adjustment strategies, called *full* (Equation [6]) and *diagonal* (Equation [14]) adjustments, were compared in terms of FA-NRMSE and residual error of the fit, computed as the average $||\mathrm{B}^{+}_{1,\mathrm{S:n}} - \mathrm{L_n B}^{+}_{1,\mathrm{ref}}||_{\mathrm{Fro}}$ over the control database. Finally, a measure of the distance of the adjustment matrix to the identity matrix was also performed with two different metrics: the L_∞ norm and the maximum coefficient over the diagonal, denoted in this work by $\mathrm{L}_{\infty,\mathrm{D}}$.

Experimental validation

Acquisitions were performed on 3 healthy volunteers (21±1 years, 1 female/2 males) on a whole-body investigative 7T MR system (Magnetom 7T, Siemens Healthcare, Erlangen, Germany) equipped with a Nova 8Tx-32Rx head coil (Nova Medical, Wilmington, MA, USA). This study was approved by the local Institutional Review Board (approval number 2018-A01761-54) and the volunteers provided informed written consent prior to examinations. Sequences were run within the Siemens protected mode, i.e. with a peak power limit per channel of 540 W, average power limits of 1.5 W per channel and 8 W total at the coil plug. For each volunteer, a second order shim was performed, then a $\Delta \mathrm{B_0}$ scan, consisting in a 3D-GRE sequence, and two B^{+}_{1} scans, consisting in interferometric turbo-FLASH sequences (16–18), were acquired: i) a fast B^{+}_{1} scan that was used for the computation of the L matrix, and ii) a full-brain B^{+}_{1} scan that was used for the correction of B^{+}_{1} inhomogeneities in $\mathrm{T_1}$ quantification based on the MP2RAGE

Table 1

	ΔB_0 **scan**	**Fast** B_1^+ **scan**	**Full-brain** B_1^+ **scan**	**MP2RAGE**
TR (ms)	8	1000	10000	5000
TEs (ms)	1.9/3.4/5.4	1.7	1.7	3.27
TIs (ms)	-	-	-	800/2700
FAs (deg)	5	1	7	4/5
Resolution	$(2.5\ \text{mm})^3$	$(5\ \text{mm})^2$	$(5\ \text{mm})^2$	$(0.8\ \text{mm})^3$
Slice number	-	3	39	-
Slice thickness (mm)	-	5	2.5	-
Slice gap	-	600%	200%	-
Acceleration†	-	-	-	3
BW (Hz/pixel)	550	878	878	240
TA	0:44	0:10	1:40	9:40

†Generalized Autocalibrating Partially Parallel Acquisitions (GRAPPA) (29) with 24 reference lines.

image pairs. Anatomical scans consisted in three MP2RAGE sequences (19, 20): the first run used the UP version of the excitation pulse, the second run the adjusted SUP, and the third run the subject-tailored one. Given the low FA-NRMSE achieved with the UP inversion, all MP2RAGE acquisitions used this inversion pulse for magnetization preparation. Hence, any difference amongst these acquisitions is expected to originate mostly from variations in the FA profile of the excitation pulse. Sequence parameters are listed in Table 1.

Uniform (UNI) contrasts were processed from the two inversion volumes of the MP2RAGE sequences using an in-house Matlab script (19, 20). T_1 maps were computed both without and with B_1^+ inhomogeneity correction using the full-brain B_1^+ maps according to the procedure introduced in (14, 21). UNI images were segmented in 5 tissue classes (grey matter, white matter, CSF, bone and soft tissues) using spm12 (R7219, http://www.fil.ion.ucl.ac.uk/spm) (25). The resulting tissue probability maps were thresholded to 5% to obtain grey matter and white matter masks.

Results

Standardised design database

Using a statistical representation of the inter-individual B_1^+ variation (15), maps of the second order statistics (i.e. mean and covariance) of the transmit RF field can be computed from a B_1^+ database as:

$$\begin{cases} \hat{\mu}_{B_1^+} = \frac{1}{N_s} \sum_{n=1}^{N_s} B_{1,S:n}^+ \\ \hat{C}_{B_1^+} = \frac{1}{N_s} \sum_{n=1}^{N_s} \left(B_{1,S:n}^+ - \hat{\mu}_{B_1^+} \right)^H \left(B_{1,S:n}^+ - \hat{\mu}_{B_1^+} \right) \end{cases} \tag{16}$$

where A^H denotes this Hermitian conjugate of A. In this study, this has been done from the 35 B_1^+ obtained by pooling the design (20 subjects) and control (15 subjects) databases. For the estimation of the variance matrix, a Ledoit-Wolf correction (26) was applied as the number of maps remained too small given the high dimensionality (8 complex variables) of the measured B_1^+ maps (the observable quantity). Not using this correction could lead to rank-deficient correlation matrices which are physically not realistic. The second order statistics estimated over the "raw" design database and the standardised design database are displayed in the Supporting Information Figure S1. While the mean transmit RF fields $\hat{\mu}_{B_1^+}$ and $\hat{\mu}_{\tilde{B}_1^+}$ (Figure S1a and b) remain very similar, it can be observed that the variance of the standardised RF field ($\hat{C}_{\tilde{B}_1^+}$) is significantly smaller than the variance of the "raw" RF field ($\hat{C}_{B_1^+}$) (Figure S1c and d). In other words, a significant part of the variance of the "raw" RF field is contained in the adjustment matrix L.

Simulation results

The FA simulation results over the control database are reported in Figures 2 and 3 for the UP, the adjusted SUP and for the subject-tailored pulses. An example of set of pulses obtained in one subject is reported in Supporting Information Figure S2. One can observe that the RF and MFG waveforms of the UP and the SUP differ significantly. The value of the pulse scaling parameter λ was generally defined by the energy per channel exceeding the 15 mW limit. The distance of the adjustment matrix to the identity matrix, as well as the pulse energy and maximal amplitude are represented in the Supporting Information Figure S3. From this figure, no clear correlation was found between the energy or the peak amplitude of the adjusted SUP and $\|L_n - I\|_\infty$. Moreover, comparing $\|L_n - I\|_\infty$ and $\|L_n - I\|_{\infty,D}$, we found that the maximum difference between L_n and I was located on the diagonal only for half of the subjects. Finally, we observe from this figure that the scaling procedure applied on the adjusted SUP to satisfied the imposed energy constraints led to an average increase of the pulse length of 25% (ranging from 0% to 50%).

The FA distributions averaged over the control database (see Equation [13]) illustrated in Figure 2a and 2b, showed an improved accuracy and spatial homogeneity with adjusted SUPs compared to UP. Interestingly, the coefficient of variation computed from Equation [13] (Figure 2c) demonstrates more reproducible FA patterns across subject using the SUP approach. This was also quantified by the histograms of the CV (Figure 2d) where values are centered

around 7% for the UP and 4% for the adjusted SUPs, both of them outperforming the CP mode. The effect of pulse rescaling (see Equation [12]) can be observed in Figure 2 by comparing the performance of the the scaled ($\text{AdjSUP}_{\text{Scaled}}$) and non-scaled ($\text{AdjSUP}_{\text{Notscaled}}$) adjusted SUPs, the latter being obtained by forcing λ to 1 and thereby presenting the risk of exceeding either of the energy or RF amplitude thresholds imposed for the excitation pulse. From the FA profiles and the histograms, we can conclude that the effect of scaling the pulse had only a minimal effect on pulse performance. Finally, the subject-tailored pulses showed excellent performances, both in terms of spatial homogeneity and inter-subject robustness.

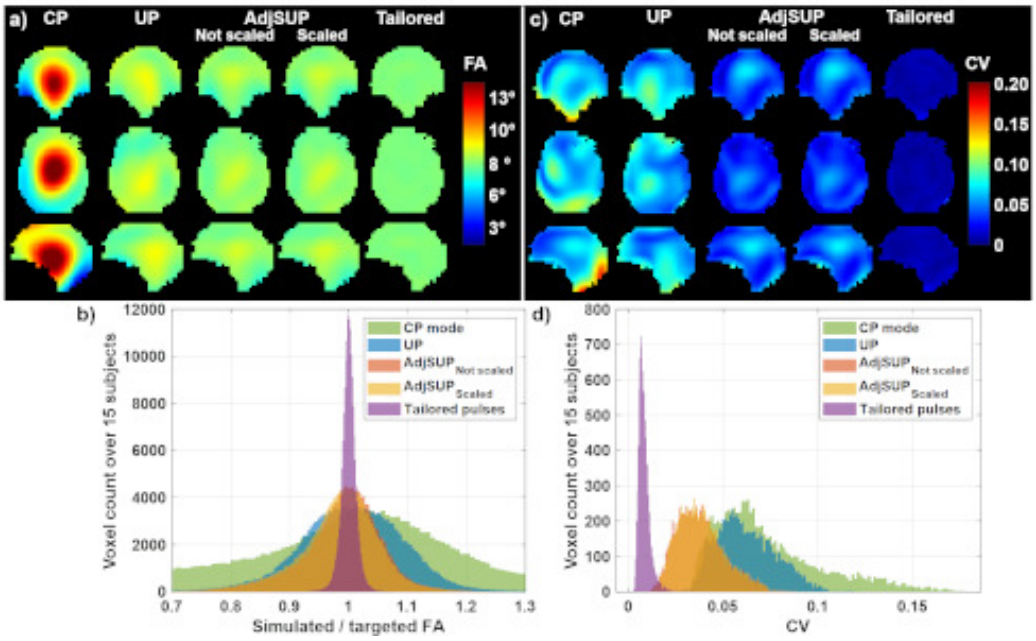

Figure 2: FA maps (obtained by numerical integration of Bloch's equation) over a control database of 15 subjects for i) an 8° hard pulse in CP mode, ii) an 8° UP, iii) an 8° SUP adjusted to the subjects ($\text{adjSUP}_{\text{Notscaled}}$), iv) the same 8° SUP adjusted scaled to match scanner and RF safety limits ($\text{adjSUP}_{\text{Scaled}}$), and v) with subject-tailored pulses. a) Coronal, axial and sagittal views of FA maps averaged over the population. b) Corresponding normalised FA-histograms showed an improvement of excitation accuracy and precision with adjusted SUPs compared to UP. c) Coronal, axial and sagittal views of coefficient of variation (CV) maps measured over the population. d) Corresponding CV-histograms showed an increased inter-subject robustness of the excitation patterns with adjusted SUPs compared to UP. The scaling only slightly decreased pulse performances.

These results translated in an improved FA-NRMSE, along with less outliers and reduced intersubject variability (Figure 3): the FA-NRMSE values were were 8.8% for the UP, 7.1% for the adjusted SUP and 1.3% for the subject-tailored pulses, on average across the 15 subjects of the control database.

A diagonal adjustment led to an increased residual error of the fit (residual error of $0.22 \pm$

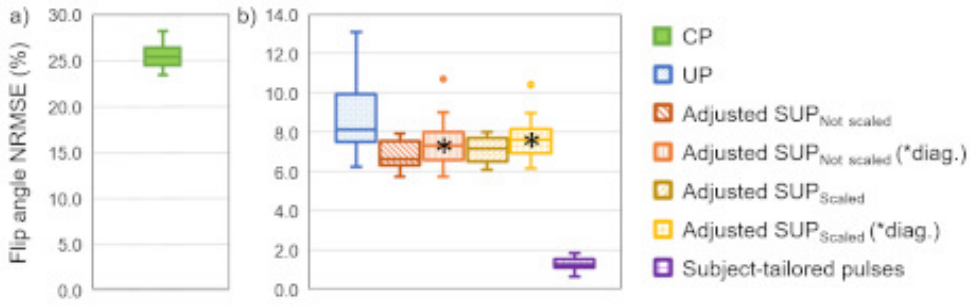

Figure 3: Boxplots of the subject-wise FA normalised root mean square error (FA-NRMSE) measured on the control database of 15 subjects for a) the hard pulse in CP mode, and b) the UP, adjSUP$_{\text{Notscaled}}$, adjSUP$_{\text{Scaled}}$ and the subject-tailored pulses. CP results were displayed in a separate boxplot as they required a different scale. Two boxplots are displayed for the adjusted SUPs: the dark-coloured ones represent the results obtained in with the full adjustment, i.e. from an adjustment matrix with off-diagonal coefficients, while the light-coloured boxplots were obtained from a diagonal adjustment. Adjusted SUPs showed improved performance compared to UP in terms of FA-NRMSE, outliers and reduced intersubject variability. The pulse scaling to satisfy scanner and SAR limits only slightly decreased pulse performance. The adjustment with a diagonal matrix lead to lower FA-NRMSE compared to the approach with off-diagonal terms.

0.04) compared to a full adjustment (0.13±0.03). In addition, the FA-NRMSE was systematically higher for the diagonal adjustment as compared to the full adjustment. A paired t-test with a significance threshold of 5% returned a p-value < 0.01. Finally, the difference between the FA-NRMSE of the adjusted SUP and the UP appeared to be statistically significant for the full adjustment (p-value of 0.01), but not for the diagonal adjustment (p-value of 0.09).

In vivo results

An axial view of the MP2RAGE UNI images acquired over the three volunteers of the study is displayed in Figure 4. UP images showed small signal inhomogeneities along the right-left and antero-posterior axis, while the signal in adjusted SUP images looked more homogeneous, and seemed occasionally to offer a better delineation between white matter and grey matter. Surprisingly, the signal obtained using subject-tailored pTX pulses for subjects 1 and 2 also showed spatial inhomogeneities in the frontal lobe. This was possibly caused by motion-induced local B_0 and B_1^+ changes between the time of acquisition of the static field offset and RF maps and the MP2RAGE sequence (approximately 30-min delay). In subject 3, where the subject-tailored MP2RAGE sequence was acquired straight after pulse design, this artefact was not present.

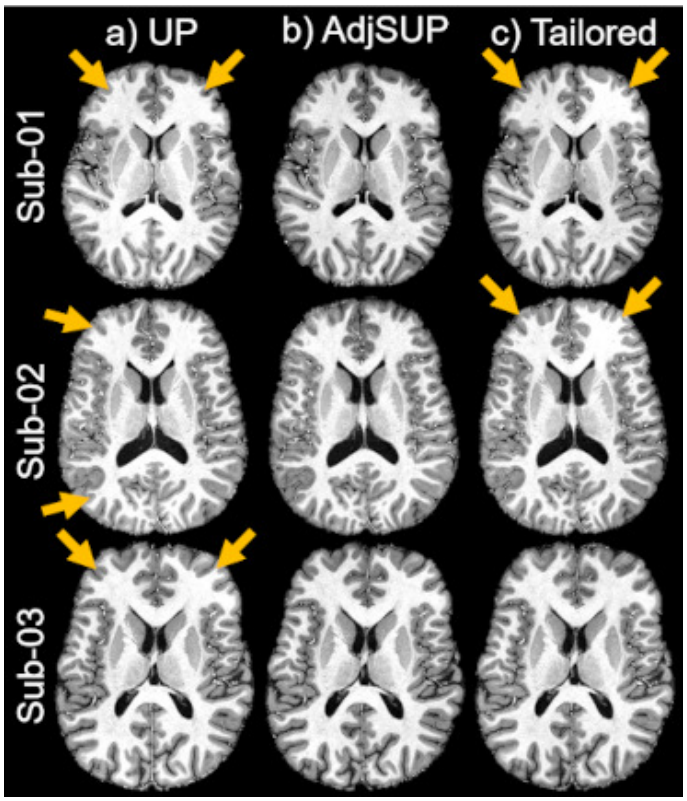

Figure 4: UNI contrasts measured for the three subjects of the study from the two inversion volumes of the MP2RAGE sequence acquired with an universal inversion pulse and an excitation a) universal pulse, b) adjusted SUP, c) subject-tailored pulse. Yellow arrows indicate signal inhomogeneities along the left/right or antero/posterior axis.

The T_1 maps measured in subject 3 without and with B_1^+ correction are presented in Figure 5. From the difference images (third row) and the associated boxplots, it can be seen that without B_1^+ correction, T_1 error can locally largely exceed 100 ms for the UP-based acquisition. That bias was reduced using the adjusted SUP, the subject-tailored pulse remaining the most accurate solution though.

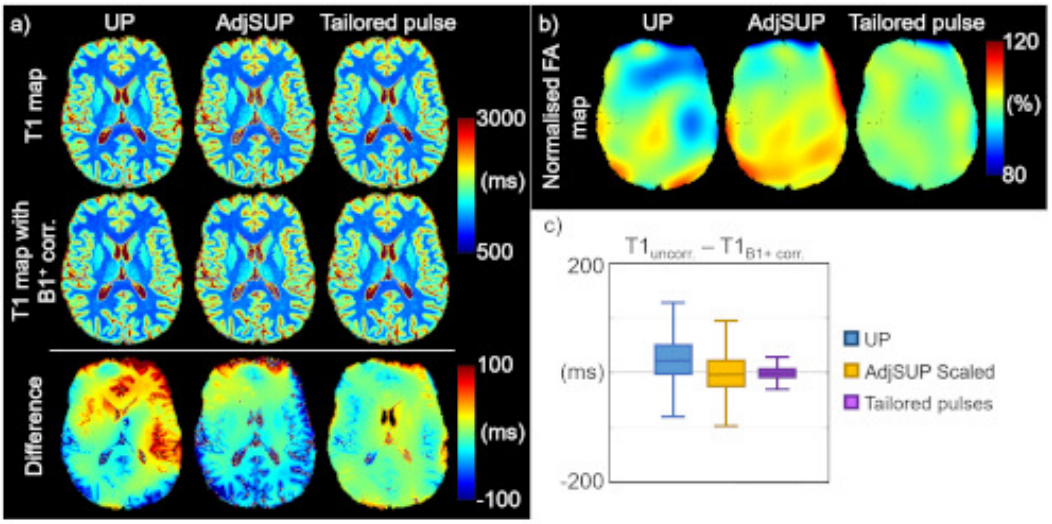

Figure 5: T_1 maps computed in subject 3 by injecting UNI signal intensities and sequence parameters in the Bloch simulator (numerical integration) for the MP2RAGE sequence acquired with a universal inversion pulse and from the left to the right: an universal excitation pulse, an adjusted SUP excitation pulse and a subject-tailored excitation pulse. T_1 maps were computed without (top line) and with (middle line) B_1^+ profile correction. b) Normalised FA maps. c) Boxplots of the difference between T1 computed without and with B_1^+ profile correction in the same subject.

The T_1 Histograms measured in the joint masks of white and grey matter (i.e. cerebrospinal fluid excluded) for each subject are presented in Figure 6. As expected from the simulations, and noting that the three participant have the same age, T_1 values were quite reproducible across subjects when measured from adjusted SUP and subject-tailored images, while UP images showed a greater inter-subject variability.

Discussion

In the current study, a new pTX UP design methodology called SUP was proposed where a set of RF and MFG waveforms is designed offline on a so-called standardized database, and the RF waveforms adjusted to the subject during the MRI session thanks to a fast calibration scan (< 10 s). For neuroimaging at 7T, UPs (and thus SUPs) provide already better homogeneity than a CP mode pulse at 3T (27) so that emphasis was put here on quantitative methods

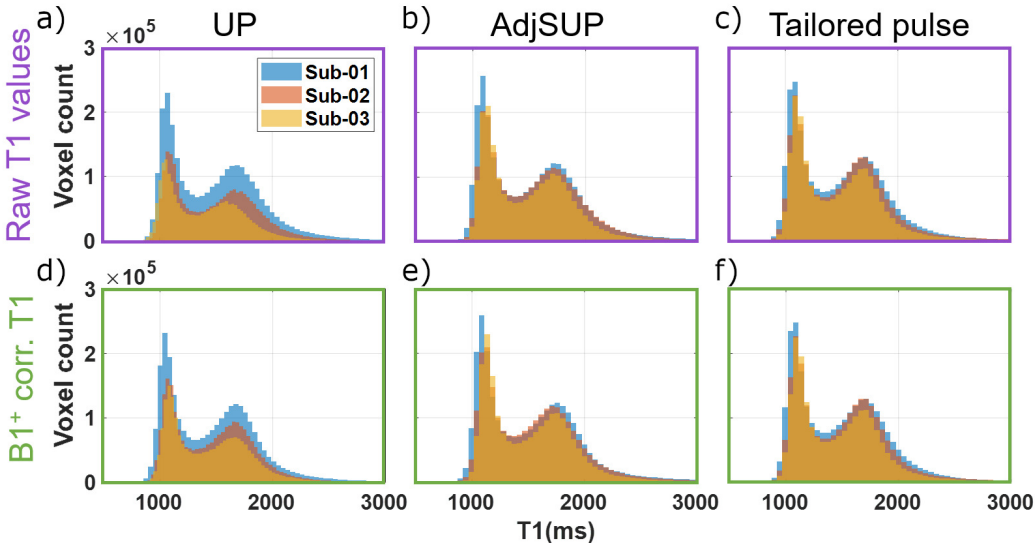

Figure 6: T_1 histograms extracted for each subject (sub-01 to sub-03) from MP2RAGE images acquired with a,d) UP, b,e) adjusted SUPs and c,f) subject-tailored pulses. T_1 values were computed either without (a-c) or with (d-f) B_1^+ correction. These results showed a limited impact of B_1^+ correction on T_1 distributions. T_1 values displayed on the histograms were restricted to the subject's white matter and grey matter masks.

(MP2RAGE). Scans at higher fields or targeting pediatric imaging, where B_1^+ variability is expected to increase, could also benefit from this method. Although the theory has been presented in the light of the small tip angle approximation, the proposed technique, potentially, could be applied to any type of RF pulses, i.e. including slice selective, large FA and refocusing pulses. For the inversion pulse however, we have observed that the gain offered by the adjusted SUPs was not significant, probably due to the already excellent FA homogeneity obtained with UPs in this non linear regime (FA-NRMSE $< 2\%$) (8).

In simulation, adjusted SUPs improved signal homogeneity in the brain as compared to the UP approach, which translated in a decreased FA-NRMSE along with a better inter-subject stability of the excitation patterns, as measured by the mean value and the coefficient of variation of the FA (Equation [13]). The quality of the MP2RAGE UNI images was very satisfactory for all RF pulse, although for some subjects a small signal asymmetry remained along the left-right and antero-posterior axis. We note here that this asymmetry was absent in the UNI images obtained from the SUP-based MP2RAGE acquisitions. The subject-tailored seemed to show a greater sensitivity to head motion, perhaps due to a decreased immunity to ΔB_0 variations (12). This weakness however could be alleviated by employing e.g. a multi-frequency band pulse optimisation (7), yet at the cost of a higher computational burden. The adjusted SUPs furthermore led to a robust T_1 quantification similar to that obtained with subject-

tailored pulses. Compared to the subject-tailored approach, the main advantage of this method thus remains the absence any pulse optimisation during the MRI session (Equation [6] being in essence a simple quadratic problem that is solved by pseudo-inverse).

In this study, we observed that the adjustment matrix can deviate significantly from the identity matrix, on the diagonal as well as off-diagonal coefficients. Furthermore, we observed that a full adjustment was superior to a diagonal adjustment, where the off-diagonal coefficients are forced to zero. This observation suggests that the variations in head positions and anatomies can lead to RF coupling variations that can be accounted for by using a full adjustment, but not a diagonal adjustment. The observed effect might be correlated with the variations of the scattering matrix of the transmitter array, which can be measured by the MR system itself, and which can be exploited for motion tracking purposes (28).

The adjustment procedure proposed in the current study can increase the pulse amplitude as well as its energy. To mitigate this problem, the pulse was scaled by a factor λ that exactly divides the pulse amplitude and energy by λ. This factor never exceeded 1.5, leading to a pulse duration increase of less than 120 μs, of minimal impact on the echo spacing of the MP2RAGE sequence. Other strategies, consisting in adding enforcing RF energy constraints in Equation [6] to avoid scaling the pulse, were envisaged but lead to a significant performance degradation.

The least-squares problem to compute the adjustment matrix is overdetermined, which allows adjusting a SUP from a subsampled B_1^+ scan that included only 3 axial slices. As such, the scan time spent to map B_1^+ was reduced compared to the subject-tailored approach, where typically a minimum of 10 to 20 slices are required (10). The putative link between the adjustment matrix and the scattering matrix of the transmitter array could be explored to eventually be able to further speed-up this pulse adjustment step. In future developments, the computation of the adjustment matrix could be implemented directly on the scanner as part of an automated calibration procedure, providing in pTX a generalisation of the reference voltage calibration available in single transmission. Here, the choice of the reference map based on which the B_1^+ maps were standardised ($B_{1,\mathrm{ref}}^+$) has an impact on the definition of the standardised database and therefore, may influence SUP performance. Although not shown in this work, we have tested the possibility of using any B_1^+ map of a particular subject of the design database as the reference $B_{1,\mathrm{ref}}^+$. All these definitions were acceptable in the sense that the mean and covariance of the FA (see Equation [13]) improved as compared to the UP. Taking the average resonant RF field seemed a better choice as it tends to eliminate the influence of a particular

B_1^+ in the database. However, we do not exclude that other (potentially better) definitions for $B_{1,\text{ref}}^+$ exist.

Finally, an interesting field of application of SUPs would be MRI of other body parts at UHF using pTX. When imaging the abdomen or the thorax, one has to face greater B_1^+ variations due to an increased variability of the morphology across subjects. In this potential field of application, it is foreseeable that the definition of the reference B_1^+ can significantly vary as compared to what has been proposed in this work. Possibly a multiplicity of references, and therefore a large amount of data, would be necessary to make the approach generalizable to other body parts (13).

In conclusion, the use of adjusted SUP has shown potential to further improve excitation profiles and inter-subject robustness as compared to the UP approach without session-specific pulse design, which simplifies the workflow compared to a subject-tailored pulse design.

Acknowledgements

This work has received financial support from Leducq Foundation (large equipment Equipement de Recherche et Plateformes Technologiques program, NEUROVASC7T project) and from FET-Open H2020 (AROMA project, grant agreement n°885876).

Conflicts of interest

Aurélien Massire is an employee of Siemens Healthineers SAS.

References

[1] Liu W, Collins CM, Smith MB. Calculations ofB 1 distribution, specific energy absorption rate, and intrinsic signal-to-noise ratio for a body-size birdcage coil loaded with different human subjects at 64 and 128 MHz. Applied magnetic resonance 2005;29:5.

[2] Katscher Ulrich, Börnert Peter, Leussler Christoph, Van Den Brink Johan S. Transmit sense. Magnetic Resonance in Medicine 2003;49:144–150.

[3] Adriany Gregor, Moortele Pierre-Francois, Wiesinger Florian, et al. Transmit and receive transmission line arrays for 7 Tesla parallel imaging. Magnetic Resonance in Medicine 2005;53:434–445.

[4] Hoult David I. Sensitivity and power deposition in a high-field imaging experiment. Journal of Magnetic Resonance Imaging 2000;12:46–67.

[5] Ibrahim Tamer S, Lee Robert, Baertlein Brian A, Kangarlu Allahyar, Robitaille Pierre-Marie L. Application of finite difference time domain method for the design of birdcage RF head coils using multi-port excitations. Magnetic resonance imaging 2000;18:733–742.

[6] Cloos MA, Boulant N, Luong M, et al. kT-points: short three-dimensional tailored RF pulses for flip-angle homogenization over an extended volume. Magnetic Resonance in Medicine 2012;67:72–80.

[7] Malik Shaihan J, Keihaninejad Shiva, Hammers Alexander, Hajnal Joseph V. Tailored excitation in 3D with spiral nonselective (SPINS) RF pulses. Magnetic resonance in medicine 2012;67:1303–1315.

[8] Van Damme L, Mauconduit F, Chambrion Thomas, Boulant N, Gras V. Universal non-selective excitation and refocusing pulses with improved robustness to off-resonance for Magnetic Resonance Imaging at 7 Tesla with parallel transmission. Magnetic Resonance in Medicine 2021;85:678–693.

[9] Brunheim Sascha, Gratz Marcel, Johst Sören, et al. Fast and accurate multi-channel mapping based on the TIAMO technique for 7T UHF body MRI. Magnetic resonance in medicine 2018;79:2652–2664.

[10] Herrler Jürgen, Liebig Patrick, Gumbrecht Rene, et al. Fast online-customized (FOCUS) parallel transmission pulses: A combination of universal pulses and individual optimization. Magnetic resonance in medicine 2021;85:3140–3153.

[11] Gras Vincent, Boland Markus, Vignaud Alexandre, et al. Homogeneous non-selective and slice-selective parallel-transmit excitations at 7 Tesla with universal pulses: A validation study on two commercial RF coils. PLoS One 2017;12:e0183562.

[12] Gras Vincent, Vignaud Alexandre, Amadon Alexis, Le Bihan Denis, Boulant Nicolas. Universal pulses: a new concept for calibration-free parallel transmission. Magnetic resonance in medicine 2017;77:635–643.

[13] Tomi-Tricot Raphaël, Gras Vincent, Thirion Bertrand, et al. SmartPulse, a machine learning approach for calibration-free dynamic RF shimming: Preliminary study in a clinical environment. Magnetic resonance in medicine 2019;82:2016–2031.

[14] Mauconduit Franck, Massire Aurélien, Gras Vincent, Amadon Alexis, Vignaud Alexandre, Boulant Nicolas. PASTeUR package extension with MP2RAGE for robust T1 mapping technique in parallel transmit at 7T. Proceedings of the Annual Meeting of ISMRM 2020;3709.

[15] Gras Vincent, Mauconduit Franck, Boulant Nicolas. A Statistical Robust Approach to Design Parallel Transmit Radiofrequency Excitations in MRI. Concepts in Magnetic Resonance Part A 2020;2020.

[16] Fautz HP, Vogel M, Gross P, Kerr A, Zhu Y. B1 mapping of coil arrays for parallel transmission. Proceedings of the Annual Meeting of ISMRM 2008;1247.

[17] Brunner David O, Pruessmann Klaas P. B1+ interferometry for the calibration of RF transmitter arrays. Magnetic Resonance in Medicine 2009;61:1480–1488.

[18] Amadon Alexis, Cloos Martijn Anton, Boulant Nicolas, Hang Marie-France, Wiggins Christopher John, Fautz Hans-Peter. Validation of a very fast B1-mapping sequence for parallel transmission on a human brain at 7T. Proceedings of the Annual Meeting of ISMRM 2012;3358.

[19] Marques José P, Kober Tobias, Krueger Gunnar, Zwaag Wietske, Moortele Pierre-François, Gruetter Rolf. MP2RAGE, a self bias-field corrected sequence for improved segmentation and T1-mapping at high field. Neuroimage 2010;49:1271–1281.

[20] Marques Jose P, Gruetter Rolf. New developments and applications of the MP2RAGE sequence-focusing the contrast and high spatial resolution R1 mapping. PloS one 2013;8:e69294.

[21] Massire Aurélien, Taso Manuel, Besson Pierre, Guye Maxime, Ranjeva Jean-Philippe, Callot Virginie. High-resolution multi-parametric quantitative magnetic resonance imaging of the human cervical spinal cord at 7T. Neuroimage 2016;143:58–69.

[22] Grissom William, Yip Chun-yu, Zhang Zhenghui, Stenger V Andrew, Fessler Jeffrey A,

Noll Douglas C. Spatial domain method for the design of RF pulses in multicoil parallel excitation. Magnetic Resonance in Medicine 2006;56:620–629.

[23] Setsompop Kawin, Wald Lawrence L, Alagappan Vijayanand, Gagoski Borjan A, Adalsteinsson Elfar. Magnitude least squares optimization for parallel radio frequency excitation design demonstrated at 7 Tesla with eight channels. Magnetic Resonance in Medicine 2008;59:908–915.

[24] Hoyos-Idrobo Andres, Weiss Pierre, Massire Aurélien, Amadon Alexis, Boulant Nicolas. On variant strategies to solve the magnitude least squares optimization problem in parallel transmission pulse design and under strict SAR and power constraints. IEEE transactions on medical imaging 2013;33:739–748.

[25] Friston Karl J, Holmes Andrew P, Worsley Keith J, Poline J-P, Frith Chris D, Frackowiak Richard SJ. Statistical parametric maps in functional imaging: a general linear approach. Human brain mapping 1994;2:189–210.

[26] Ledoit Olivier, Wolf Michael. A well-conditioned estimator for large-dimensional covariance matrices. Journal of multivariate analysis 2004;88:365–411.

[27] Boulant N, Mangin J-F, Amadon A. Counteracting radio frequency inhomogeneity in the human brain at 7 Tesla using strongly modulating pulses. Magnetic Resonance in Medicine 2009;61:1165–1172.

[28] Hess Aaron T, Tunnicliffe Elizabeth M, Rodgers Christopher T, Robson Matthew D. Diaphragm position can be accurately estimated from the scattering of a parallel transmit RF coil at 7 T. Magnetic resonance in medicine 2018;79:2164–2169.

[29] Griswold Mark A, Jakob Peter M, Heidemann Robin M, et al. Generalized autocalibrating partially parallel acquisitions (GRAPPA). Magnetic Resonance in Medicine 2002;47:1202–1210.